Materials Physics and Mechanics 40 (2018) 7-11 Received: May 22, 2018

A SIMPLIFIED MODEL EXPLAINING THE FORMATION OF InAs NANOWIRES ON GaAs NANOMEMBRANES

V.G. Dubrovskii

ITMO University, Kronverkskiy pr. 49, 197101 St. Petersburg, Russia

e-mail: dubrovskii@mail.ioffe.ru

Abstract. Gold-free GaAs nanomembranes have proven ideal templates for further growth of in-plane III-V nanowires. Recently, it has been demonstrated that high quality InAs nanowires with a low defect density can be obtained on top of GaAs nanomembranes by molecular beam epitaxy in wafer-scale approach and provide an excellent platform for future investigations into one-dimensional transport and quantum computation. Here, we develop a model to explain why InAs NWs form spontaneously on the top ridges of GaAs nanomembranes and not elsewhere. We speculate that the driving force for this growth mechanism is the free energy minimization including the elastic and surface energy contributions.
Keywords: InAs nanowires, GaAs nanomembranes, elastic stress relaxation, growth model

1. Introduction

Highly mismatched InAs/GaAs material system (lattice mismatch $\varepsilon_0 = 0.07$) has been used for a long time for epitaxial growth of the Stranski-Krastanow quantum dots [1, 2]. This material system is also very useful for growing high quality axial [3] and radial [4] heterostructures in vertical nanowires (NWs). More recently, defect-free GaAs nanomembranes (NMs) have been used as templates for further III-V NW growth [5, 6]. Such structures have been successfully grown by metalorganic chemical vapour deposition and molecular beam epitaxy (MBE) using a gold-free selective area approach [5 – 7]. The NMs are patternable at the wafer scale and can additionally be fabricated in the form of Y-shaped structures [6, 8]. In Ref. [8], it has been shown that InAs NWs form on the top ridges of GaAs NMs with a certain shape and aspect ratio. Such structures are scalable and provide electron confinement to the top NWs which is sufficient to produce quasi-one-dimensional conduction. Here, we present a simplified model to explain the experimentally observed morphology of the NW/NM structures.

2. Model

The InAs/GaAs NW/NM structure is shown in Fig. 1 (a) [8] and is fabricated as follows. First, <11-2>-aligned GaAs NMs are grown by selective area approach as described in Ref. [5]. These NMs have a sharp top restricted by (-11-3) and (-1-31) planes, and vertical (01-1) and (0-11) sidewalls. Then, InAs is deposited by MBE for 200 s at 540°C and accumulated at the top of the NMs, forming InAs NWs along the NM vertex. The InAs NWs are restricted by two vertical (01-1) and (0-11) sidewalls, two (-11-3) and (-1-31) planes parallel to the NM ridges, and flat (111) top. Our aim is to understand and explain this shape of InAs NWs and in particular the experimentally observed aspect ratio $x = h/l$ of about 0.6 [8].

http://dx.doi.org/10.18720/MPM.4012018_2

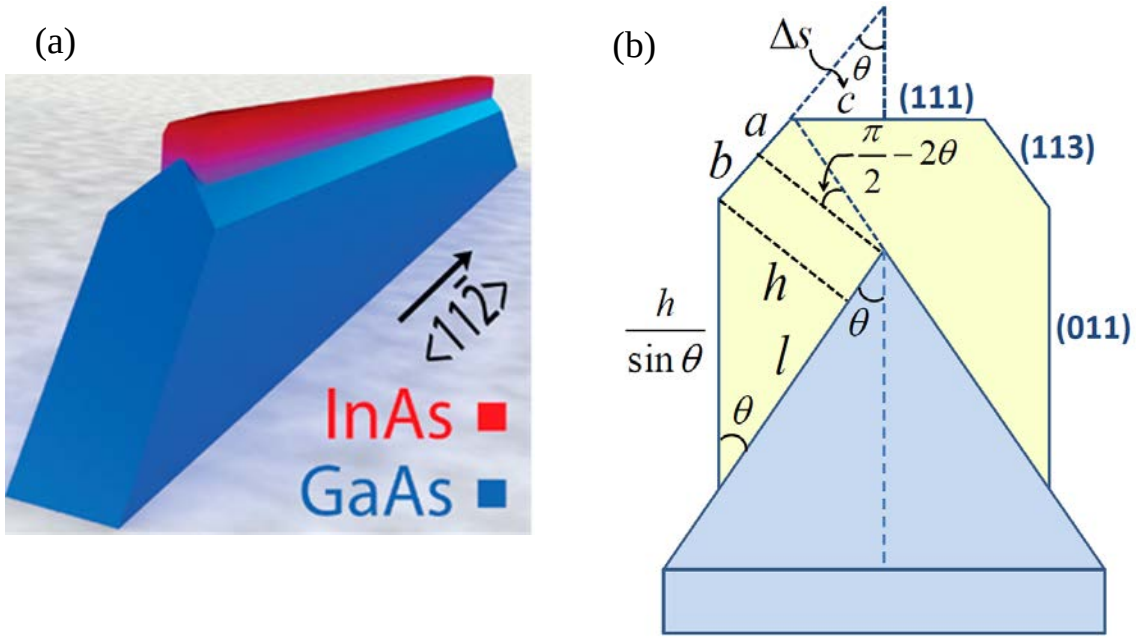

Fig. 1. (a) Morphology of a single GaAs/InAs NM/NW structure [8], and (b) plan view of the model geometry showing the relevant parameters

According to the data [8], the InAs NW facets are composed of vertical, horizontal and inclined facets of the (011), (111) and (113) families, respectively (see Fig. 1 (b)). We additionally assume that the inclined NW facets are replaced by the horizontal facets at the crossing point of the initial NM facets with the inclined NW facets. From geometrical considerations, we have $a = h\cot an2\theta$ and $b = l - h\cot an\theta$, with θ as the taper angle of the NM, hence

$$b + a = l - h(\cot an\theta - \cot an2\theta). \quad (1)$$

The (131) facet of the InAs NW of width $b + a$ and surface energy $\gamma_{InAs}^{(131)}$ replaces the initial facet of the GaAs NM of width l and surface energy $\gamma_{GaAs}^{(131)}$. Additionally, the NW formation creates the InAs-GaAs interface of width l and interfacial energy $\gamma_{InAs-GaAs}^{(131)}$. We also create the vertical facet of height $h/\sin\theta$ having the surface energy $\gamma_{InAs}^{(011)}$, and the horizontal facet of width c and surface energy $\gamma_{InAs}^{(111)}$. From geometrical considerations,

$$c = h\frac{\sin\theta}{\sin 2\theta}. \quad (2)$$

Summarizing all these surface energy terms and using $\mathrm{cotan}2\theta = (1/2)(\mathrm{cotan}\theta - \tan\theta)$ and $\sin\theta = 2\sin\theta\cos\theta$ in Eqs. (1) and (2), respectively, the surface energy change per the length $2d$ (where d is the length of the initial NM) equals

$$\Delta F_{surf} = \left[\gamma_{InAs-GaAs}^{(131)} + \gamma_{InAs}^{(131)} - \gamma_{GaAs}^{(131}\right]l + \left[\frac{\gamma_{InAs}^{(011)}}{\sin\theta} - \frac{1}{2}\gamma_{InAs}^{(131)}(\tan\theta + \cot an\theta) + \frac{\gamma_{InAs}^{(111)}}{2\cos\theta}\right]h. \quad (3)$$

Grouping the bracket terms into C_1 and C_2, we can write

$$\Delta F_{surf} = C_1 l + C_2 h. \quad (4)$$

Clearly, the C_1 term gives the surface energy change in the (131) direction and is positive in the non-wetting and negative in the wetting cases, respectively. The C_2 term should always be positive and is associated with the InAs facets in contact with vapor.

The surface area of half the NW cross-section s equals the area of the parallelogram lh minus the area of the upper triangle Δs. The latter is given by $h^2/(8\sin\theta\cos\theta)$. Therefore,

$$s = lh - \frac{h^2}{8\sin\theta\cos\theta}, \tag{4}$$

where the second term is less than 10% of the first one in our geometry and can be neglected in the first approximation.

To account for the effect of the strain relaxation, we use the simplest formula [9 – 11]

$$\Delta G_{elastic} = \lambda\varepsilon^2 V \frac{1}{1+\alpha h/l}, \tag{5}$$

showing that the elastic energy (for the reduced strain ε due to dislocations) rapidly decreases ($\alpha >> 1$) with increasing the aspect ratio h/l with respect to the 2D film of the same volume V. These dislocations are seen at the InAs/GaAs interface, with a density of ~ 100/μm of length, reducing the lattice mismatch to $\varepsilon \cong 0.03$ [8].

Using $V \cong 2dlh$ and dividing Eq. (5) to the facet length $2d$, we arrive at the equation expressing the free energy $\Delta F = \Delta F_{surf} + \Delta F_{elastic}$ [with $\Delta F_{elastic} = \Delta G_{elastic}/(2d)$] of forming InAs NW of width l and height h on top of the GaAs NM

$$\Delta F(l,h) = C_1 l + C_2 h + \frac{C_3 lh}{1+\alpha h/l}. \tag{6}$$

This free energy is defined per unit length of the structure. The C_1 term gives the surface energy change upon covering the GaAs (131) facets with InAs, and is proportional to the NW width l. The C_2 term ($C_2 > 0$) stands for the surface energy of all other InAs facets, and is proportional to the NW height h. The last term gives the elastic energy of InAs NW, proportional to the NW cross-sectional area $s \cong lh$, with C_3 being the elastic energy per unit volume for the reduced mismatch [9], and α describing the stress relaxation with the aspect ratio h/l [9 – 11]. We also assume that the term associated with the dislocation energy is roughly the same for any aspect ratio, which should be valid for large enough volumes of deposited InAs with the NW heights already well above the critical thickness for forming misfit dislocations (~1.2 nm).

3. Results and discussion

To access the preferred shape of InAs on top of GaAs, we minimize the formation energy given by Eq. (6) in h at a fixed $s \cong lh = const$, corresponding to a fixed volume of deposited InAs [12]. Using $l = s/h$, Eq. (6) can be re-arranged in terms of h only:

$$\Delta F(h) = C_1 \frac{s}{h} + C_2 h + \frac{C_3 s}{1+\alpha h^2/s}. \tag{7}$$

It is interesting to note that the derivative of this free energy with respect to h depends solely on the aspect ratio $x = h/l$. Introducing $f = \Delta F/C_2$ (C_2 is always positive), we obtain

$$\frac{df}{dh} = 1 - \frac{A}{x} - \frac{v x^{1/2}}{(1+\alpha x)^2}. \tag{8}$$

Here, $A = C_1/C_2$ is the normalized surface energy change in the (131) plane, which is positive in the non-wetting and negative in the wetting case, and $v = 2\alpha(C_3/C_2)s^{1/2}$ is the strain-induced factor that increases with the amount of deposited InAs per unit area s. The preferred aspect ratio is now defined by the stable zero point of df/dh corresponding to the minimum free energy.

Figure 2 shows two possible cases with the preferred $x \cong 0.6$, as observed experimentally in Ref. [6]. Of course, the three-dimensional (3D) geometry will occur in the non-wetting case with $A > 0$ even without any lattice mismatch, because the surface energy minimization leads to a reduction of the energetically costly InAs-GaAs interface [11]. This is shown by the dashed curve in Fig. 2. We believe, however, that our GaAs/InAs system is initially wetting. Therefore, the surface energy favours two-dimensional (2D) growth of InAs on GaAs, while 3D structures emerge only after the formation of a continuous wetting layer, as in the Stranski-Krastanow growth [11]. The energetics of the system is then described by the solid line in Fig. 2. In this case, reaching a high aspect ratio on the order of 0.6, which is necessary to form the NWs on top of the NMs, can only be due to strain relaxation and requires a high value of the strain-induced coefficient v of about 140. The C_3 coefficient equals $\lambda\varepsilon^2$, with $\lambda = 1.22 \times 10^{11}$ J/m^3 as the elastic modulus of InAs and ε as the reduced lattice mismatch. With the experimentally observed ε = 0.03, this yields $v = 140$ at α = 15 (Ref. [10]) for a plausible value of $C_2 = 0.091$ J/m^2.

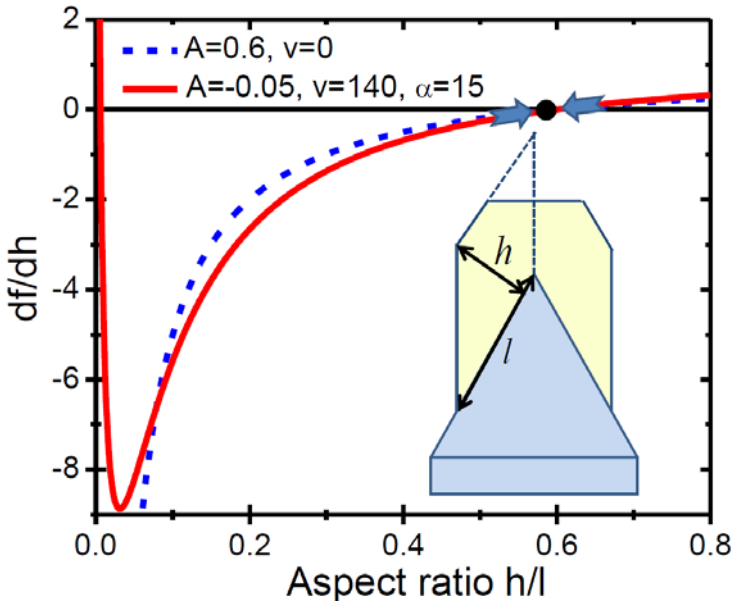

Fig. 2. Derivative of the free energy of forming InAs NW on GaAs NM with respect to the aspect ratio, obtained from Eq. (8) in the non-wetting ($A > 0$) and wetting ($A < 0$) case

The zero point at $h/l \cong 0.6$ corresponds to the minimum free energy of forming the NW, because its derivative is negative for smaller and positive for larger aspect ratios. The real curve is expected to be the one in the wetting case, where the system surpasses an energetic barrier at a small x as in the Stranski-Krastanow growth. The value of $v = 140$ corresponds to the parameters of InAs with the reduced mismatch ε =0.03. The insert shows the geometry, the approximation $s \cong lh$ used in the calculations neglects truncation of the full parallelogram in the top NW part.

4. Conclusions

In conclusion, our model shows that formation of InAs NWs on the top ridges of GaAs NMs is driven by minimization of the formation energy including the surface and elastic contributions. In the wetting case, relevant for this material system, the existence of the optimal aspect ratio of InAs NWs ~ 0.6 can only be due to the elastic energy relaxation with the reduced strain. This energy minimum follows from the model with plausible parameters.

We now plan to consider other material systems, including a very promising case of InSb, using similar methods. It is also interesting to study in more detail the nucleation stage [13], growth kinetics of in-plane III-V NWs on the NM templates [14], and in particular three-fold symmetrical Y-shaped structures.

Acknowledgements*. The author thanks the Ministry of Education and Science of the Russian Federation for financial support under grant 14.587.21.0040 (project ID RFMEFI58717X0040).*

References

[1] L. Goldstein, F. Glas, J.Y. Marzin, M.N. Charasse, G. Le Roux // *Applied Physics Letters* **47** (1985) 1099.
[2] D. Bimberg, M. Grundmann, N.N. Ledentsov, *Quantum dot heterostructures* (Wiley, New York, 1999).
[3] V. Zannier, D. Ercolani, U.P. Gomes, Je. David, M. Gemmi, V.G. Dubrovskii, L. Sorba // *Nano Letters* **16** (2016) 7183.
[4] K.W. Ng, W.S. Ko, T.-T. D. Tran, R. Chen, M.V. Nazarenko, F. Lu, V.G. Dubrovskii, M. Kamp, A. Forchel, C.J. Chang-Hasnain // *ACS Nano* **7** (2013) 100.
[5] G. Tutuncuoglu, M. de la Mata, D. Deiana, H. Potts, F. Matteini, J. Arbiolbe, A. Fontcuberta i Morral // *Nanoscale* **7** (2015) 19453.
[6] Z. Yang, A. Surrente, G. Tutuncuoglu, K. Galkowski, M. Cazaban-Carrazé, F. Amaduzzi, P. Leroux, D.K. Maude, A. Fontcuberta i Morral, P. Plochocka // *Nano Letters* **17** (2017) 2979.
[7] C.-Y. Chi, C.-C. Chang, S. Hu, T.-W. Yeh, S.B. Cronin, P.D. Dapkus // *Nano Letters* **13** (2013) 2506.
[8] M. Friedl, K. Cerveny, P. Weigele, G. Tütüncüoglu, S. Marti-Sanchez, C. Huang, T. Patlatiuk, H. Potts, Z. Sun, M.O. Hill, L. Güniat, W. Kim, M. Zamani, V.G. Dubrovskii, J. Arbiol, L.J. Lauhon, D.M. Zumbühl, A. Fontcuberta i Morral // *Nano Letters* **18** (2018) 2666.
[9] F. Glas // *Physical Review B* **74** (2006) 121302.
[10] X. Zhang, V.G. Dubrovskii, N.V. Sibirev, X. Ren // *Crystal Growth & Design* **11** (2011) 5441.
[11] V.G. Dubrovskii, N.V. Sibirev, X. Zhang, R.A. Suris // *Crystal Growth & Design* **10** (2010) 3949.
[12] V.G. Dubrovskii, V. Consonni, A. Trampert, L. Geelhaar, H. Riechert // *Physical Review B* **85** (2012) 165317.
[13] V.G. Dubrovskii, J. Grecenkov // *Crystal Growth & Design* **15** (2015) 340.
[14] Q. Gao, V.G. Dubrovskii, P. Caroff, J. Wong-Leung, L. Li, Y. Guo, Lan Fu, H.H. Tan, C. Jagadish // *Nano Letters* **16** (2016) 4361.